DIS on nuclei using holography

based on
1808.01952 and 1807.07969 with Ismail Zahed

Kiminad Mamo (Stony Brook U.)

Nov 14, 2018 @ INT, *Seattle*

Outline

Outline

Outline

Outline

Motivation

- the EMC collaboration and others at CERN, and SLAC have made a surprising observation that the structure function of iron differs substantially from that of the deuteron

Motivation

- the EMC collaboration and others at CERN, and SLAC have made a surprising observation that the structure function of iron differs substantially from that of the deuteron
- why would scattering at high energy and momentum transfer be affected by intra-nuclear effects that are much lower in energy?

Motivation

- the EMC collaboration and others at CERN, and SLAC have made a surprising observation that the structure function of iron differs substantially from that of the deuteron
- why would scattering at high energy and momentum transfer be affected by intra-nuclear effects that are much lower in energy?
- we examine the role of strong coupling when the nuclear many-body system is probed electromagnetically in the DIS limit

Motivation

- the EMC collaboration and others at CERN, and SLAC have made a surprising observation that the structure function of iron differs substantially from that of the deuteron
- why would scattering at high energy and momentum transfer be affected by intra-nuclear effects that are much lower in energy?
- we examine the role of strong coupling when the nuclear many-body system is probed electromagnetically in the DIS limit
- for dilute nuclei with small atomic number A, the leading contribution is on one-nucleon state smeared by Fermi motion which should be justified in the large-x region. We estimate the DIS scattering on the few-nucleon amplitudes using holography

Motivation

- the EMC collaboration and others at CERN, and SLAC have made a surprising observation that the structure function of iron differs substantially from that of the deuteron
- why would scattering at high energy and momentum transfer be affected by intra-nuclear effects that are much lower in energy?
- we examine the role of strong coupling when the nuclear many-body system is probed electromagnetically in the DIS limit
- for dilute nuclei with small atomic number A, the leading contribution is on one-nucleon state smeared by Fermi motion which should be justified in the large-x region. We estimate the DIS scattering on the few-nucleon amplitudes using holography
- shadowing in the small-x regime is currently understood as the coherent scattering on two or more nucleons in the nucleus, as opposed to incoherent scattering on individual nucleons

Motivation

- the EMC collaboration and others at CERN, and SLAC have made a surprising observation that the structure function of iron differs substantially from that of the deuteron
- why would scattering at high energy and momentum transfer be affected by intra-nuclear effects that are much lower in energy?
- we examine the role of strong coupling when the nuclear many-body system is probed electromagnetically in the DIS limit
- for dilute nuclei with small atomic number A, the leading contribution is on one-nucleon state smeared by Fermi motion which should be justified in the large-x region. We estimate the DIS scattering on the few-nucleon amplitudes using holography
- shadowing in the small-x regime is currently understood as the coherent scattering on two or more nucleons in the nucleus, as opposed to incoherent scattering on individual nucleons
- we consider DIS scattering on a large but finite nucleus in holography using an extremal RN-AdS black-hole. This point of view takes to the extreme the concept of coherent DIS scattering on a dense nucleus, and therefore should be of relevance in the shadowing or low-x region

DIS on a Dilute Nucleus

- we consider deep inelastic scattering (DIS) on a nucleus described using a density expansion as

$$\frac{\mathcal{G}_A^{\mu\nu}}{\langle P_A|P_A\rangle} = \int dN\, \mathcal{G}_N^{\mu\nu} + \frac{1}{2!}\int dN_1\, dN_2\, \mathcal{G}_{2N}^{\mu\nu} + \ldots$$

DIS on a Dilute Nucleus

- we consider deep inelastic scattering (DIS) on a nucleus described using a density expansion as

$$\frac{\mathcal{G}_A^{\mu\nu}}{\langle P_A | P_A \rangle} = \int dN \, \mathcal{G}_N^{\mu\nu} + \frac{1}{2!} \int dN_1 \, dN_2 \, \mathcal{G}_{2N}^{\mu\nu} + \ldots$$

with the connected DIS amplitudes

$$\mathcal{G}_{nN}^{\mu\nu} = i \int d^4 z \, e^{iq\cdot z}$$
$$\times \langle N(p_1) \ldots N(p_n) \, | [J^\mu(z), J^\nu(0)] | \, N(p_1) \ldots N(p_n) \rangle_c$$

DIS on a Dilute Nucleus

- we consider deep inelastic scattering (DIS) on a nucleus described using a density expansion as

$$\frac{\mathcal{G}_A^{\mu\nu}}{\langle P_A|P_A\rangle} = \int dN\,\mathcal{G}_N^{\mu\nu} + \frac{1}{2!}\int dN_1\,dN_2\,\mathcal{G}_{2N}^{\mu\nu} + \ldots$$

with the connected DIS amplitudes

$$\mathcal{G}_{nN}^{\mu\nu} = i\int d^4z\,e^{iq\cdot z} \times \langle N(p_1)\ldots N(p_n)\,|[J^\mu(z),J^\nu(0)]|\,N(p_1)\ldots N(p_n)\rangle_c$$

and the nucleon phase-space occupation factors

$$dN_i = 4\,\frac{d^3r_i}{V_3}\,\frac{d^3p_i}{(2\pi)^3}\,\frac{1}{2E_{p_i}}\,\mathbf{n}(r_i,p_i)$$

for unpolarized neutrons and protons

DIS on a Dilute Nucleus

- the leading density contribution is

$$\frac{\mathcal{G}_A^{\mu\nu}}{\langle P_A|P_A\rangle} \approx \rho_0 \frac{4\pi}{3} R_A^3 \int \frac{d^3p}{2V_3 E_p} \frac{\theta(p_F - |\vec{p}|)}{\frac{4}{3}\pi p_F^3} \mathcal{G}_p^{\mu\nu}$$

$$+16\pi \int_{R_A}^{R_A+\Delta} r^2 dr \int \frac{d^3p}{(2\pi)^3} \frac{1}{2V_3 E_p} \theta(p_F(r) - |\vec{p}|) \mathcal{G}_p^{\mu\nu}$$

DIS on a Dilute Nucleus

- the leading density contribution is

$$\frac{\mathcal{G}_A^{\mu\nu}}{\langle P_A|P_A\rangle} \approx \rho_0 \frac{4\pi}{3} R_A^3 \int \frac{d^3p}{2V_3E_p}\, \frac{\theta(p_F - |\vec{p}|)}{\frac{4}{3}\pi p_F^3}\, \mathcal{G}_p^{\mu\nu}$$
$$+16\pi \int_{R_A}^{R_A+\Delta} r^2 dr \int \frac{d^3p}{(2\pi)^3} \frac{1}{2V_3E_p} \theta(p_F(r) - |\vec{p}|)\, \mathcal{G}_p^{\mu\nu}$$

with the DIS scattering on a single nucleon

$$\begin{aligned} \mathcal{G}_p^{\mu\nu} &= F_1^p(x_p, q^2)\, (\eta^{\mu\nu} - \hat{q}^\mu \hat{q}^\nu) \\ &+ \frac{2x_p}{q^2}\, F_2^p(x_p, q^2) \left(p^\mu + \frac{1}{2x_p} q^\mu\right) \left(p^\nu + \frac{1}{2x_p} q^\nu\right) \end{aligned}$$

and the nucleon 3-momentum is fixed by Fermi motion with $x_p = -q^2/2q \cdot p$ and tied to x by

$$\frac{x}{x_p} = \frac{E_p}{m_N} - \frac{|\vec{p}|}{m_N} \cos\theta_p$$

Here $x = -q^2/2\omega m_N$ is Bjorken-x for a free nucleon at rest

DIS on a Nucleon using Holography

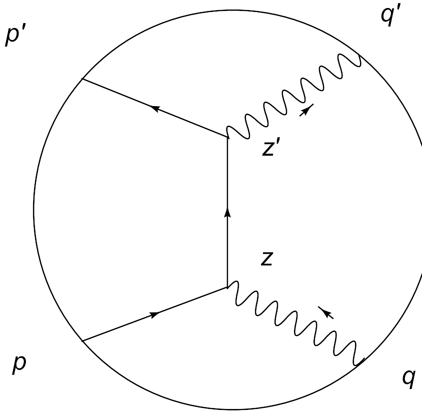

Figure: s-channel Compton scattering

DIS on a Nucleon using Holography

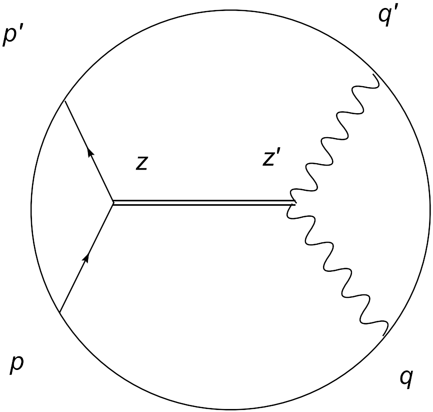

Figure: t-channel graviton exchange

DIS on a Nucleon using Holography

- in holography, Compton scattering on a nucleon at the boundary maps onto the scattering in bulk of the R-current onto a dilatino with spin-1/2 at large-x, while at small-x the same scattering is dominated by the t-exchange of a closed string, with the interpolating result

$$F_2^p(x,q^2) =$$
$$\tilde{\mathbb{C}}\left(\frac{m_N^2}{-q^2}\right)^{\tau-1}\left(x^{\tau+1}(1-x)^{\tau-2}+\mathbb{C}\left(\frac{m_N^2}{-q^2}\right)^{\frac{1}{2}}\frac{1}{x^{\Delta_{\mathbb{P}}}}\right)$$

with $mR = 3/2$ or $\tau = \Delta - 1/2 = 3$

R-ratio

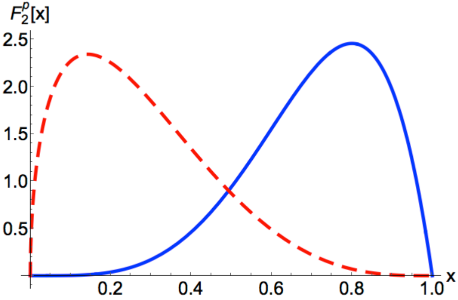

Figure: Large-x dependence of the nucleon structure function $F_2^p[x]$ for weak coupling (dashed curve) and strong coupling (solid curve) normalized to 1.

R-ratio

- the R-ratio

$$
\begin{aligned}
R[x,q^2] \approx \int \frac{d^3p}{1+3\epsilon_A} \\
\Bigg[\left(\frac{\theta(p_F - |\vec{p}|)}{\frac{4}{3}\pi p_F^3} + \frac{3\kappa_A}{2} \frac{\theta(p_S - |\vec{p}|)}{\frac{4}{3}\pi p_S^3} \right) \\
\times \frac{3x_p E_A}{2x_A E_p} \left(\left(\frac{E_A E_p + \frac{-q^2}{4x_A x_p}}{E_A^2 + \frac{-q^2}{4x_A^2}} \right)^2 - \frac{1}{3} \frac{m_N^2 + \frac{-q^2}{4x_p^2}}{E_A^2 + \frac{-q^2}{4x_A^2}} \right) \\
\times \frac{x_p^a (1-x_p)^b + \mathbb{C} \left(\frac{m_N^2}{-q^2} \right)^{\frac{1}{2}} \frac{1}{x_p^c}}{x^a (1-x)^b + \mathbb{C} \left(\frac{m_N^2}{-q^2} \right)^{\frac{1}{2}} \frac{1}{x^c}} \Bigg]
\end{aligned}
$$

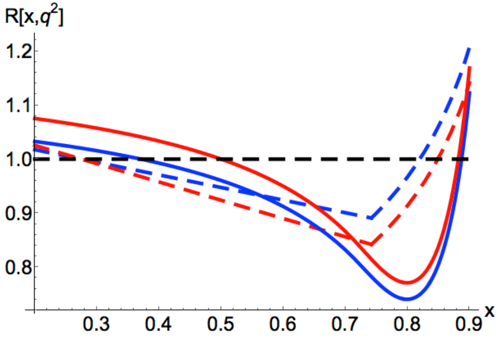

Figure: R-ratio at large-x using the leading density contribution and the holographic nucleon structure function (solid curves), versus the parametrized empirical ratio (dashed curves), for $A = 12$ (blue curves) and $A = 42$ (red curves).

DIS on a Dense Nucleus

DIS on a Dense Nucleus

- DIS on thermal black hole in AdS was initiated by Hatta, Iancu, and Mueller in 2007

DIS on a Dense Nucleus

- DIS on thermal black hole in AdS was initiated by Hatta, Iancu, and Mueller in 2007
- we consider deep inelastic scattering (DIS) on a large nucleus described as an extremal RN AdS black hole

$$ds^2 = \frac{r^2}{R^2}\left(-f\,dt^2 + d\vec{x}^2\right) + \frac{R^2}{r^2 f} dr^2$$

with

$$f(r) = \left(1 - \frac{r_+^2}{r^2}\right)\left(1 - \frac{r_-^2}{r^2}\right)\left(1 + \frac{r_+^2}{r^2} + \frac{r_-^2}{r^2}\right)$$

DIS on a Dense Nucleus

- an extremal RN AdS black hole has the EoS

$$s = \frac{2\pi}{\sqrt{3}}\sqrt{\alpha}n$$
$$\epsilon = \frac{3}{4}n\mu = 3p$$
$$n = \frac{N_c^2}{96\pi^2\alpha^2}\mu^3$$

- we identify the extremal RN-AdS black hole with a very large but finite nucleus of volume $V_A = \frac{4}{3}\pi R_A^3$ with a radius $R_A = R_1 A^{\frac{1}{3}}$, a number density $A/V_A = n$, energy density $E_A/V_A = \epsilon$, and an energy per particle $E_A/A = \frac{3}{4}\mu$ (conformal). For comparison, nuclear matter with small scattering lengths carries $E_A/A \sim \frac{3}{5}\mu$ (free massive fermions), while neutron matter with large scattering lengths carries $E_A/A \sim \frac{3}{4}\mu$ close to the conformal limit.

DIS on a Dense Nucleus

- to probe the RN-AdS black hole in bulk, we use the U(1) R-field $\mathbf{A}_\mu(x)$ as the source of the *fermion* bilinear 4-vector current in the boundary of AdS_5 ($r = \infty$), and

$$\mathbf{J}_\mu(q) = G^R_{\mu\nu}(q)\, \mathbf{A}^\nu(-q)$$

with the retarded Green's function

$$G^R_{\mu\nu}(q) = -i \int d^4y\, e^{iq\cdot y} \left\langle J_\mu(y) J_\nu(0) \right\rangle_R$$

- which can be decomposed as

$$\begin{aligned} G^R_{\mu\nu}(x_A, q^2) &= \left(\eta_{\mu\nu} - \frac{q_\mu q_\nu}{Q^2}\right) R_1(x_A, q^2) \\ &+ \left(n_\mu - \frac{n\cdot q}{Q^2} q_\mu\right)\left(n_\nu - \frac{n\cdot q}{Q^2} q_\nu\right) R_2(x_A, q^2) \end{aligned}$$

DIS on a Dense Nucleus

- with

$$x_A = \frac{q^2}{-2q\cdot(nE_A)} \equiv \frac{Q^2}{2E_A\omega} = \frac{xm_N}{E_A}$$

- the DIS structure functions of the RN-AdS black hole will be identified from the imaginary part of the retarded response function

$$2\pi F_1 = \mathrm{Im} R_1 \qquad 2\pi F_2 = \frac{\omega}{E_A}\,\mathrm{Im} R_2$$

DIS on a Dense Nucleus

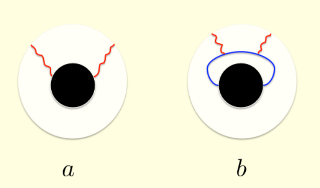

Figure: Absorptive virtual-photon scattering on a nucleus as an extremal RN-AdS black hole: (a) absorptive tree contribution; (b) absorptive one-loop contribution.

DIS on a Dense Nucleus

- the retarted response function is extracted from the induced action $\mathcal{S}[A]$ as a functional of the boundary fields $A_\mu(t,x,0)$ using

$$G^R_{\mu\nu}(q) \;=\; \frac{\partial^2 \mathcal{S}_R}{\partial A_\mu \partial A_\nu}\bigg|_{A_\mu = A_{\mu(u=0)}}$$

- we find the on-shell boundary action

$$\mathcal{S}_R = \quad -\frac{1}{\alpha}\frac{N_c^2\gamma^2\mu^2}{48}\Bigg[k^2\mathcal{A}_L^2(0)\left(2\left(c+\ln\frac{k}{3\overline{\gamma}^2}\right)-i\pi\right) + \frac{9\pi}{\Gamma^2(\frac{1}{3})}\left(\frac{k}{3\overline{\gamma}^2}\right)^{\frac{2}{3}}\left(\frac{1}{\sqrt{3}}-i\right)\mathcal{A}_T^2(0)\Bigg]$$

DIS on a Dense Nucleus

- the holographic structure functions are

$$
\begin{aligned}
F_T(x_A, Q^2) &= C_T\,\frac{\mu^2}{x_A}\,\left(\frac{x_A^2 Q^2}{\mu E_A}\right)^{\frac{2}{3}} \\
F_L(x_A, Q^2) &= C_L\,\frac{E_A}{\mu}\,\frac{\mu^2}{x_A}\,\left(\frac{x_A^2 Q^2}{\mu E_A}\right)
\end{aligned}
$$

with

$$
C_T = \frac{N_c^2}{2^{17/3}\pi^2\Gamma^2(1/3)\alpha^{5/3}}
$$

$$
C_L = \frac{N_c^2}{1152\pi^4\alpha^2}
$$

and $F_2 = F_L + F_T \simeq F_T = 2x_A F_1$ (approximate Callan-Gross relation)

DIS on a Dense Nucleus

- normalization

$$(2\pi)^3\,2E_A\,\delta(\vec{0}_p) \equiv \,2E_A\,V_A \to (12\pi\alpha)^2\frac{A^2}{N_c^2\mu^2}$$

- the properly normalized structure functions at low-x

$$\begin{aligned} F_T^A(x,Q^2) &= \tilde{C}_T\,\frac{A}{x}\,\left(\frac{3x^2Q^2}{4m_N^2}\right)^{\frac{2}{3}} \\ F_L^A(x,Q^2) &= \tilde{C}_L\,\frac{3A}{4x}\left(\frac{3x^2Q^2}{4m_N^2}\right) \end{aligned}$$

with $\tilde{C}_{T,L}/C_{T,L} = \pi^5(48\alpha)^2/2N_c^2$

DIS on a Dense Nucleus

- the R-ratio is

$$R[x] \equiv \frac{\frac{1}{A}F_2^A}{F_2^N} = \qquad \frac{\tilde{C}_T}{C_\Delta}\,\frac{x^{\Delta_{\mathbb{P}}+\frac{1}{3}}}{x_S^{2\Delta-\frac{8}{3}}}\left(1+\frac{3\tilde{C}_L}{4\tilde{C}_T}\left(\frac{x}{x_S}\right)^{\frac{2}{3}}\right)$$

with $x_S \equiv 2m_N/\sqrt{3}Q$

DIS on a Dense Nucleus

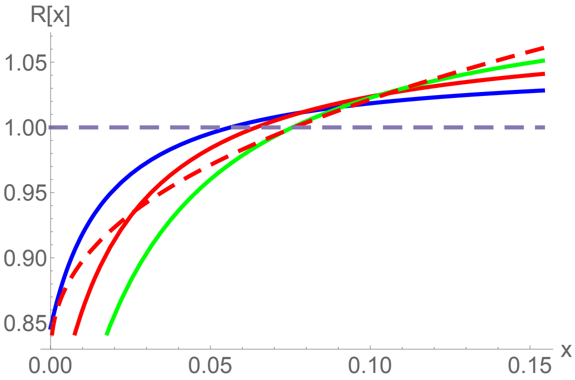

Figure: Parametrized DIS data on nuclei (solid curves) vs holography (dashed curve) in the shadowing region.

2. Summary and Conclusion

- we have used the holographic structure functions for DIS scattering on single nucleons to make a non-perturbative estimate of the nuclear structure function of dilute nuclei
- and we have found that the leading contribution is on one-nucleon state smeared by Fermi motion which compares well with the data in the large-x region
- we have described a dense nucleus as an extremal RN-AdS black hole
- and using its R-current correlators we have determined the structure functions as a function of Bjorken-x
- the R-ratio of the nuclear structure functions of the extremal RN-AdS black hole exhibit strong shadowing at low-x

Thank You!